THE JOURNAL OF PHYSICAL CHEMISTRY B

Article

pubs.acs.org/JPCB

Hydrophobic and Hydrophilic Associations of a Methanol Pair in Aqueous Solution

Manik Kumer Ghosh, Nizam Uddin, and Cheol Ho Choi*

Department of Chemistry and Green-Nano Materials Research Center, College of Natural Sciences, Kyungpook National University, Taegu 702-701, South Korea

ABSTRACT: The association dynamics of a methanol pair in aqueous solution were theoretically studied with QM/EFP-MD and quantum mechanical methods. Stable contact pairs and solvent separated configurations (**SS**) were found from simulations with a free energy barrier of 2 kcal/mol, revealing the strong tendency of methanol association. The stable contact pairs were further identified as the hydrophobic ($\mathbf{CP_A}$) and hydrophilic ($\mathbf{CP_B}$) species, with the $\mathbf{CP_A}$ having a larger population. Although the free energy difference between the $\mathbf{CP_A}$ and $\mathbf{CP_B}$ is negligible with virtually no associated free energy barrier, the slow isomerization dynamics of intermolecular rotations ensures their individual identity. Further mechanistic analysis revealed that only the $\mathbf{CP_A}$ has a direct path to the **SS**, showing that hydrophobic attraction initiates the association process. A subsequent intermolecular hydrophilic attraction isomerizes $\mathbf{CP_A}$ and $\mathbf{CP_B}$. Therefore, our results show that both the hydrophobic and hydrophilic attractions between methanol molecules play important roles in the association dynamics. The former operates on the longer intermolecular distance, while the latter is effective in contact pairs.

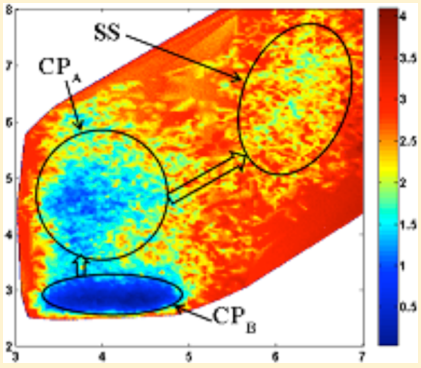

I. INTRODUCTION

The hydrophobic effect represents the tendency of apolar groups to associate in aqueous solutions.[1,2] The accommodation of apolar groups in aqueous solutions increases the associated free energy, which is due to the structural changes in the solvent around each apolar group (*hydrophobic hydration*). Those apolar groups tend to associate with each other, since it reduces the unfavorable hydrophobic surface area (*hydrophobic attraction*). It is the molecular driving force behind numerous important biological processes, including protein folding and the biological membrane formations.[1,3] Therefore, a quantitative understanding of hydrophobic interactions and its associated mechanism is crucial for modeling biological systems in aqueous solutions.[4] Despite the basic principles behind the hydrophobic effect being qualitatively well understood, the quantitative aspects of the solute and solvent interplays are largely dependent on the nature of molecular systems.

One of the consequential phenomena of hydrophobicity is the nonideal behavior of alcohol/water binary mixtures. It is well-known that thermodynamic and kinetic properties, such as entropy increase, compressibility, and mean molar volume, for these mixtures, are smaller than what would be expected for an ideal mixture of pure liquids.[1,2,5] These were initially attributed to the significant *hydrophobic hydration effect* such as the immobilized "super-structuring" of water or the formation of an ice-like structure in the surrounding water.[1,3,6,7] However, various experimental and computational studies showed that, at least at low solute concentration around room temperature, the structure and dynamics of the water molecules in the solvation shell is similar to that of bulk water.[4,8−20] Therefore, the nonideal behavior of alcohol/water binary mixtures can be better attributed to the *hydrophobic attraction*. A neutron diffraction study by Dixit et al.[21] provided strong evidence that the unusual behavior of water−methanol mixtures is due to the "incomplete mixing" at the molecular level and the retention of the bulk water network structure. Their study showed that the addition of water to methanol has the net effect of pressing methyl groups closer together, while pushing the hydroxyl groups apart, and also that the local structure of water in a water−methanol mixture is very similar to that in pure water. Using X-ray spectroscopy, Guo et al.[22] also suggested the incomplete alcohol−water mixing in which water molecules are bridging chains or rings comprising 6−8 methanol molecules. Their results confirm that methanol molecules in solution persist in structures similar to those found in their pure liquid. Clustering processes of alcohol/water "incomplete mixing" can be complex, since alcohol has both hydrophobic methyl and hydrophilic hydroxyl groups. Therefore, the association of alcohol in aqueous solution cannot simply be described by the *hydrophobic attraction* alone. In principle, the association of alcohol can yield both hydrophobic and hydrophilic contact pairs, as shown in Scheme 1. However, the exact nature of those contact pairs and their association mechanisms in aqueous solution has not been well understood.

Theoretically, using the general effective fragment potential (EFP2) method and second-order perturbation theory (MP2),[23] Adamovic and Gordon[24] studied the formation process of methanol−water mixtures adopting the cluster

Received: September 8, 2012
Revised: November 6, 2012
Published: November 19, 2012

   dx.doi.org/10.1021/jp308936g | *J. Phys. Chem. B* 2012, 116, 14254−14260

Scheme 1

HO-R ····· R-OH	R-OH ····· HO-R
Hydrophobic association(CP_A)	*Hydrophilic association*(CP_B)

models of $((MeOH/H_2O)_n$, n = 2, 3, ..., 8). Although they showed that, for all of these clusters, "incomplete mixing" was observed at the molecular level, clear hydrophobic associations of methanol were not predicted. Considerable effort has been devoted to the dynamic aspects of hydrophobic interactions and hydration by using classical Lennard–Jones potentials and various water models.[25−27] However, a classical molecular dynamics (MD) study by Wensink et al.[1,2,28] concluded that, although classical potentials for water and alcohol can reproduce experimental bulk properties of pure liquids, they cannot describe mixtures quantitatively, indicating that quantum mechanical descriptions are necessary for the quantitative understandings of hydrophobicity. Although Car–Parrinello molecular dynamics (CPMD)[1,3,29] simulations on the methanol in water[4,14,20] were performed, their main focus was not the "incomplete mixing".

It has been known from the classical MD[5,30] that simulations for 100–200 ps are necessary to obtain converged hydration dynamics. Although *ab initio* molecular dynamics (AIMD) simulations such as CPMD[6,7,29] or FMO-MD[8−20,31] can provide the most direct tool for studying "incomplete mixing", AIMD simulations over such time scales for systems with sufficient size are still difficult. To overcome this challenge, the quantum mechanical/molecular mechanical (QM/MM) method is often utilized.[21,32] As an advanced approach, the classical MM force field can be replaced with the quantum mechanically driven force field. Gao and co-workers developed an explicit polarization (X-Pol) model.[22,33,34] In this case, an entire system is divided into multiple fragments. Each fragment is treated quantum mechanically, while interfragment electrostatic interactions are treated approximately using a QM/MM framework. A similar fragment-based potential, known as EFP (effective fragment potential),[23,35] was theoretically proposed by Gordon and co-workers. The EFP consists of both the long- and short-range terms that are defined by using a perturbation theory. In the EFP approach, each water molecule is represented as a fragment of fixed geometry with a set of parameters deduced from *ab initio* calculations. In the original implementation,[24,36] called EFP1, the interaction energy between water molecules consists of Coulomb, polarization, and repulsion terms. The Coulomb term is evaluated using classical multipoles up to octupoles that are centered at each atom and at bond midpoints. To account for short-range charge-penetration effects, the charge-based terms in the Hamiltonian are augmented by damping functions. The fragment polarization energy is evaluated by considering the interaction of induced dipoles of each fragment with the static field due to the Coulomb multipoles as well as the induced field due to the induced dipoles of the other fragments. The induced dipoles are located at the centroids of localized molecular orbitals (LMO) at which (anisotropic) distributed polarizability tensors are placed. The remaining contribution to the *ab initio* EFP interactions accounts for exchange-repulsion and charge transfer effects, which is modeled in the form of Gaussian functions. The hybrid QM/EFP method has been successfully applied to the water structures,[25−27,37,38] chemical reactions,[39,40] and photochemistry in water.[41] It was shown that the EFP could successfully reproduce full QM results with comparatively low computational cost.[35] Therefore, one clear advantage of EFP as compared to classical parameters is its chemical accuracy in the calculations of energies and structures. The applicability of the hybrid QM/EFP to a long-time MD simulation of chemical reaction in aqueous solution has been recently examined,[42] where it was found that the QM/EFP-MD yields accurate free energy change and barrier associated with the transition from the zwitterion to the nonionized form of glycine in aqueous solution. This also demonstrated that sufficient sampling such as ∼100 ps is necessary to properly describe the local hydrogen bonding dynamics.

In this paper, we investigate the association processes of a methanol pair in aqueous solution both with the QM/EFP-MD simulations on a solvated methanol pair and quantum mechanical calculations on model clusters. The association mechanisms of methanol in aqueous solution and their corresponding local hydrated structures are our prime interests, which would provide us new insight of hydrophobicity and "incomplete mixing" phenomena.

II. COMPUTATIONAL DETAILS

In order to understand the stable structures and their relative energies, *ab initio* calculations on the clusters of $(MeOH)_2(H_2O)_x$, where x = 0, 1, and 2, were performed with the MP2/6-31G(d,p) level of theory.[23] A spherical system of two methanol molecules surrounded by 400 water molecules was prepared for the QM/EFP-MD simulations. The two methanol molecules and waters are treated with HF/6-31G(d) and EFP1, respectively. In order to prevent evaporation of waters during long time simulations, we applied a harmonic restraint potential with a force constant of 2 kcal/mol/Å^2 for the boundary solvent molecules as implemented in CHARMM.[43]

In order to study the methanol association process, umbrella samplings along the two carbon atoms (r_{CC}) of the two methanol molecules were performed with the harmonic constraint potential of

$$V = \frac{k}{2}(r_{CC} - r_0)^2 \quad (1)$$

Simulations on seven windows of r_0 = 3.0, 4.0, 5.0, 6.0, 7.0, 8.0, and 9.0 Å were performed to cover the reaction path from contact pairs to dissociation. The force constant (k) of 2 kcal/mol/Å^2 was used for the umbrella sampling constraints. The one-dimensional potentials of mean force (PMF) from the umbrella samplings were obtained using the weighted histogram analysis method (WHAM).[44] Initially, NVT runs of QM/EFP-MD simulations over 50 ps were performed on each of the seven windows at 300 K to equilibrate the systems. Then, QM/EFP-MD production runs over 100 ps, also in the NVT ensemble and at 300 K, were continued from the final structures after the equilibration. A two-dimensional PMF along r_{CC} and r_{OO} (the O–O distance of hydroxyl oxygen) was also generated using the seven windows by assuming zero umbrella sampling force constant along the r_{OO}. The statistical error of our simulations was estimated by the square of cumulative statistical error, as suggested by Zhu and Hummer.[45] The estimated square of cumulative error in the our calculated free energy is 0.10 kcal/mol, which is a good indication of converted PMF.

dx.doi.org/10.1021/jp308936g | J. Phys. Chem. B 2012, 116, 14254−14260

A modified version of GAMESS was used to run the QM/EFP-MD simulations. (The recent distribution of GAMESS contains these modifications.)

III. RESULTS AND DISCUSSION

A. Intermolecular Potential of Mean Force (PMF) of a Methanol Pair. With the help of CPMD[29] simulations, Li et al.[46] obtained the PMF along the hydrophobic association of a methane pair in water and found that the strength and shape of the potential of mean force are in conflict with earlier classical force-field simulations,[26,27] indicating that classical force-fields underestimate the hydrophobic attractions. In the case of methanol, both hydrophobic (methyl) and hydrophilic (hydroxyl) groups exist, which has more complex intermolecular interactions than methane, requiring accurate and balanced descriptions of both interactions. As described in the Computational Details section, we performed QM/EFP-MD simulations with umbrella sampling along the distance between the two carbon atoms (r_{CC}) of a methanol pair. The resulting PMF is presented in Figure 1. A stable contact pair is found near the methanol−methanol contact separation at 3.7 Å, while a shallow second potential minimum occurs for the solvent-separated configuration around 7 (**SS**) Å. The global minimum at 3.7 Å is more stable than the separation by 0.9 kcal/mol, which clearly indicates the tendency of hydrophobic attraction between methanol molecules in aqueous solution, providing a direct evidence of the "incomplete mixing" theory. After careful examinations, two minima of contact pair centering at 3.7 and 4.3 Å were identified. They may represent the CP_A and CP_B, as indicated in the figure. In order to further investigate the existence of two species, the PMF along the intermolecular angle ($O_2-C_1-C_3$) was calculated and is presented in Figure 2. The black, blue, and red PMFs of intermolecular angles correspond to the umbrella sampling windows of 3, 4, and 5 Å C−C distances, respectively. Two distinct minima around 60 and 130° appear, clearly indicating the existence of two different species at these short C_2-C_4 distances. In order to obtain detailed structural information, *ab initio* cluster calculations on model systems were performed in the next section.

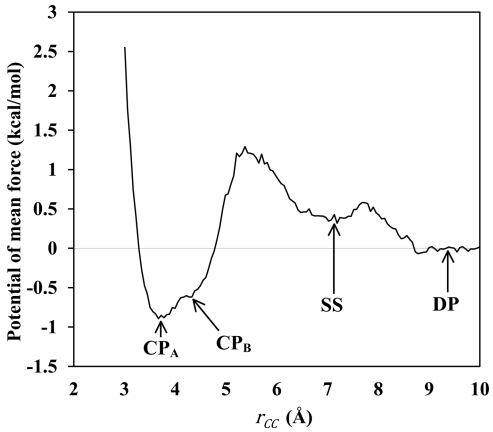

Figure 1. The potential of mean force (PMF) along the carbon−carbon distance (r_{CC}) of the methanol pair as obtained with QM/EFP-MD simulations. The **CP_A**, **CP_B**, **SS**, and **DP** represent hydrophobic contact, hydrophilic contact, solvent separated, and dissociated pairs, respectively. A spherical system of two quantum methanol molecules surrounded by 400 EFP water molecules was used. NVT simulations on seven umbrella sampling windows were performed for 100 ps at 300 K. The volume entropy corrections were done on the resulting PMF.

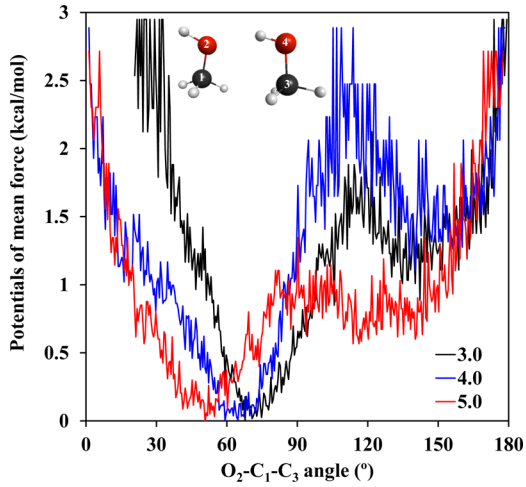

Figure 2. The potential of mean force (PMF) along the intermolecular angle ($O_2-C_1-C_3$) of the methanol pair as obtained with QM/EFP-MD simulations. The black, blue, and red PMFs of intermolecular angles correspond to the umbrella sampling windows of 3, 4, and 5 Å C−C distances, respectively.

As compared to the methane in water,[46] where no apparent free energy barrier between minima exists, our PMF of a methanol pair indicates a free energy barrier of 2 kcal/mol at r_{CC} = 5.4 Å. Therefore, both thermodynamics and kinetic environments play important roles in methanol association in water. The origin of this barrier shall be discussed in section C.

B. Quantum Mechanical Studies on the Stable Methanol Conformers. Since the intermolecular C−C (r_{CC}) and O−O (r_{OO}) distances of a static methanol pair can provide the local structural information, quantum mechanical calculations on model clusters with MP2/6-31G(d,p) were performed. Four lowest optimized structures of $(MeOH)_2$ are presented in Figure 3. They correspond to hydroxyl hydrogen bonded (**3a** and **3b**), hydroxyl-methyl hydrogen bonded (**3c**), and van der Waals dimers (**3d**), respectively, with the **3a** being

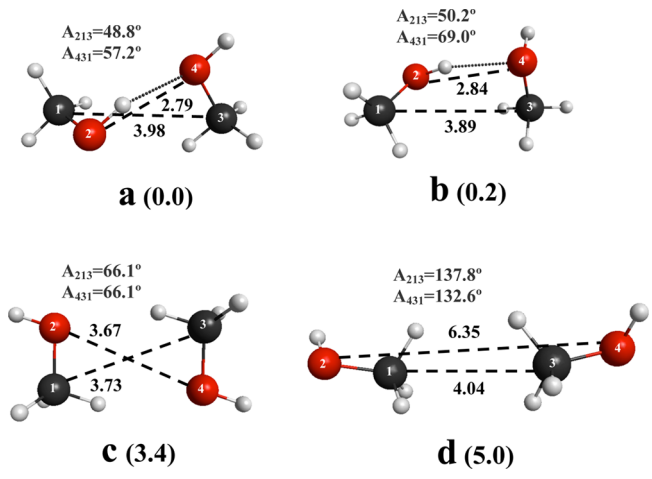

Figure 3. Fully optimized structures and relative energies of $(MeOH)_2$. All calculations were done with MP2/6-31G(d,p). The numbers in parentheses are relative energies. The distances and energies are in Å and kcal/mol, respectively.

dx.doi.org/10.1021/jp308936g | J. Phys. Chem. B 2012, 116, 14254−14260

the most stable conformer. The r_{CC} and r_{OO} of the **3a** and **3b** are nearly identical with each other. The main structural difference between **3a** and **3b** comes from the torsional angles (C−O···O−C, τ_{inter}) of 112.7 and 88.2°, respectively. The r_{OO} of **3c** and **3d** become much longer, since the hydroxyl hydrogen bonds are not present. However, the associated r_{CC} of **3c** and **3d** are not significantly changed as compared to **3a** and **3b**. The **3a** and **3b** are nearly isoenergetic and are more stable than the **3c** and **3d**, due to the hydroxyl hydrogen bonding. The typical intermolecular angles ($O_2-C_1-C_3$ and $O_4-C_3-C_1$) of the four isomers are around 60 and 130°, which are in perfect agreement with the two angles from our QM/EFP-MD, supporting the existence of two species (CP_A and CP_B) in real solution. The angles of 60 and 130° correspond to the hydrogen bonded hydrophilic and hydrophobic dimers, respectively. The optimized structures of $(MeOH)_2H_2O$ are presented in Figure 4. Except for the ring formations by the

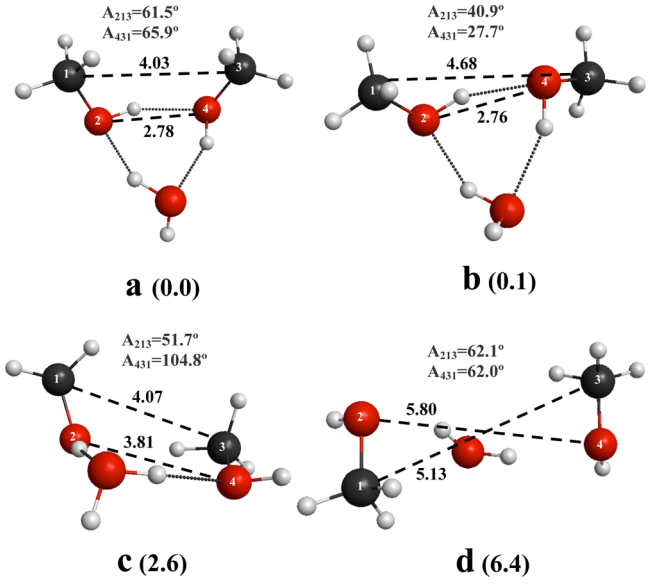

Figure 4. Fully optimized structures and relative energies of $(MeOH)_2H_2O$. All calculations were done with MP2/6-31G(d,p). The numbers in parentheses are relative energies. The distances and energies are in Å and kcal/mol, respectively.

additional water, **4a** and **4b** have similar dimer structures to those found in **3a** and **3b**. The r_{OO} of **4a** and **4b** are slightly reduced by the additional water, while the r_{CC} are somewhat increased especially in **4b**. Therefore the additional water molecule affects the hydrophobic methyl interactions more. The **4a** and **4b** are almost isoenergetic, indicating that the elongated r_{CC} in **4b** has little effect on the stabilities. The **4c** and **4d** represent the insertion of a water molecule into the hydroxyl r_{OO}, yielding slightly less stable structures. Therefore, it is seen that the methanol molecules prefer the direct hydrogen bonding using their own hydroxyl groups. Consequently, the intermolecular angle around 130°, which represents a hydrophobic dimer, does not appear in Figure 4. The water molecule inserted structures may represent the solvent separated configurations (**SS**) found in PMF (see Figure 1). Finally, the optimized structures of $(MeOH)_2(H_2O)_2$ are presented in Figure 5. Two additional water molecules form a four membered ring in **5a**, while they are inserted in the hydroxyl hydrogen bonding in **5b**. Although these two structures are more stable than the other two

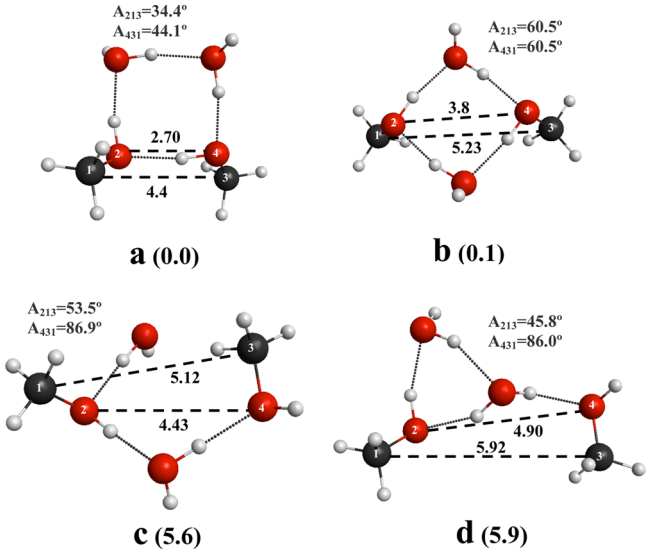

Figure 5. Fully optimized structures and relative energies of $(MeOH)_2(H_2O)_2$. All calculations were done with MP2/6-31G(d,p). The numbers in parentheses are relative energies. The distances and energies are in Å and kcal/mol, respectively.

structures, **5a** and **5b** may not be major species in real solution due to their low entropy structures. The **5c** and **5d** represent the water insertions to the hydroxyl hydrogen (r_{OO}) as found in **4c** and **4d**.

In summary, the quantum mechanical structure calculations show that the typical r_{OO} distance is 2.8 Å, when there is a hydroxyl hydrogen bond. The direct contact distance (r_{CC}) of the two methyl groups is about 4.0 Å. As the number of water molecule increases, the r_{CC} gradually increases. The intermolecular angles around 60 and 130° turned out to represent the hydrogen bonded hydrophilic and hydrophobic dimers, respectively. As a result of multiple hydrogen bondings in the most stable conformations with one and two additional water molecules, the methyl groups tend to be separated with each other, staying mostly outside of the clusters. The tendency of hydroxyl groups gathering inside of the cluster with water molecules is a direct consequence of full geometry optimizations. One may conclude that this tendency represents the "incomplete mixing" of a binary mixture of methanol and water. However, it does not show any evidence of the hydrophobic associations. Furthermore, the full geometry optimization process simply removes entropic effects. Therefore, the tendency found in quantum cluster calculations does not represent dynamic structures in real solutions. However, they do provide the first-order understanding of local structures of a methanol pair in water. On the basis of the quantum mechanical structures, our MD simulations are further analyzed in the next section.

C. Two-Dimensional (r_{CC} and r_{OO}) PMF of a Methanol Pair. On the basis of quantum mechanical calculations on model clusters, which provided the basic understanding of intermolecular angles and distances, the snapshots of MD trajectories were analyzed, and the two major species were presented in Figure 6. The species in parts a and b correspond to the hydrophilic and hydrophobic dimers, as found in the quantum mechanical calculations. The snapshots in Figure 6 as well as the static structures of Figures 3, 4, and 5 emphsize that both r_{CC} and r_{OO} are needed to clearly characterize the methanol contact pairs. Two-dimensional PMF was obtained

dx.doi.org/10.1021/jp308936g | J. Phys. Chem. B 2012, 116, 14254−14260

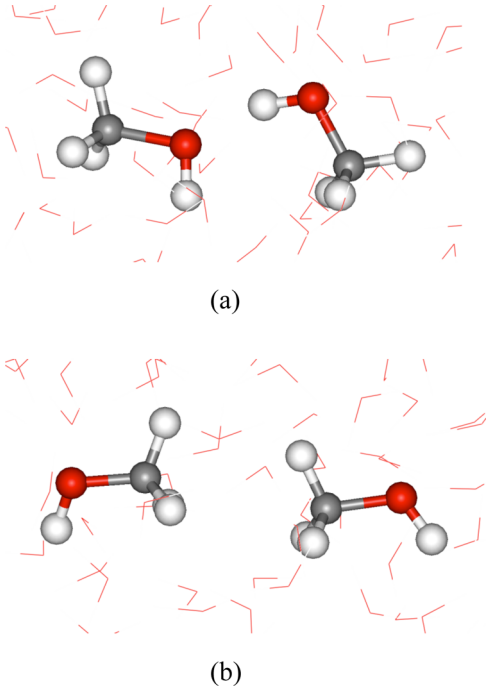

Figure 6. The major species of an umbrella sampling window of 4 Å C−C distance.

on the basis of one-dimensional umbrella sampling windows along r_{CC}, and the result is presented in Figure 7. The hydroxyl

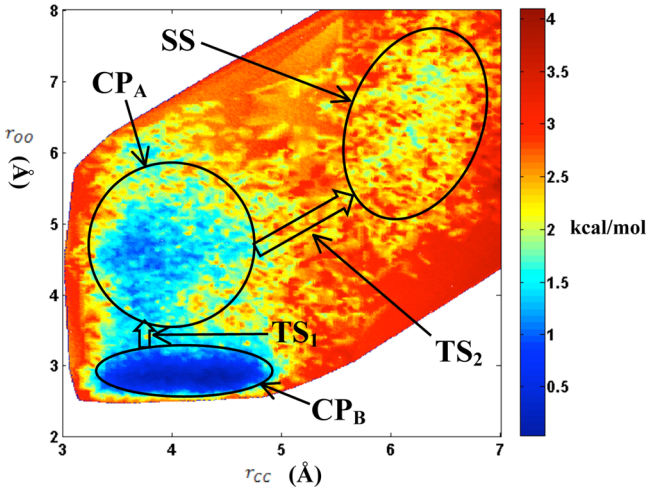

Figure 7. Two-dimensional potential of mean force (PMF) along the r_{CC} and r_{OO} of the methanol pair as obtained with QM/EFP-MD simulations. The $\mathbf{CP_A}$, $\mathbf{CP_B}$, and **SS** and represent hydrophobic contact, hydrophilic contact, and solvent separated pairs, respectively. The transition state $\mathbf{TS_1}$ connects the $\mathbf{CP_A}$ and $\mathbf{CP_B}$, while the $\mathbf{TS_2}$ connects the $\mathbf{CP_A}$ and **SS**.

oxygen (r_{OO}) distance of the two methanols was chosen as an additional coordinate for the two-dimensional PMF. The overall association mechanism of a methanol pair is also summarized in Scheme 2. A deep minimum with a narrow r_{OO} distribution around 2.8 Å (denoted as $\mathbf{CP_B}$) is seen in the lower left corner of the 2D PMF. The corresponding r_{CC} distances are 3.2−5 Å. The narrow distribution of r_{OO} distance around 2.8 Å indicates the direct hydroxyl hydrogen bondings of a methanol pair. Therefore, $\mathbf{CP_B}$ can be safely identified as hydrophilic

Scheme 2

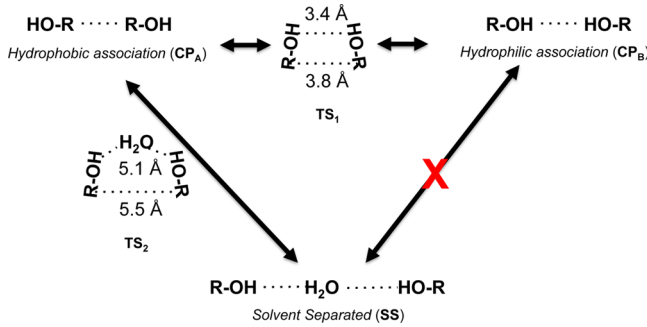

structures such as those found in **3a** and **3b**. Furthermore, the averaged r_{CC} of $\mathbf{CP_B}$ is 4.2 Å, which is close to the $\mathbf{CP_B}$ of Figure 1. On the other hand, the r_{OO} and r_{CC} distances of the region specified as $\mathbf{CP_A}$ are 3.5−6.5 and 3.2−5 Å, respectively. These distances correlate well with those of the van der Waals complex of **3c** and **3d**. The r_{CC} and r_{OO} of the deepest position of $\mathbf{CP_A}$ in PMF are around 3.6 and 4.6 Å, respectively. The r_{CC} distance of 3.6 Å is well correlated with the global minimum of the 1D PMF of Figure 1. Since there are no clear preferences of both r_{OO} and r_{CC} distances in $\mathbf{CP_A}$, neither the direct hydrogen bonding between the two-hydroxyl groups nor the clear preference of the r_{CC} distance exists. It also verified that the direct methyl group attraction of $\mathbf{CP_A}$ is structurally not as specific as the direct hydrogen bondings of $\mathbf{CP_B}$, showing that the local structures of $\mathbf{CP_A}$ are more strongly determined by solvent configurations rather than the direct solute−solute interactions. A mild transition state ($\mathbf{TS_1}$) connecting $\mathbf{CP_A}$ and $\mathbf{CP_B}$ appears at around 3.8 (r_{CC}) and 3.4 (r_{OO}) Å with nearly no free energy barrier. However, the interconversion between $\mathbf{CP_A}$ and $\mathbf{CP_B}$ requires rather significant intermolecular rotation with respect to each other. One can view this event as the conversion between **3d** and **3a** structures of Figure 3. Such molecular rotation may take ∼10 ps in water solution, necessitating sufficient samplings for the correct dynamics. Consequently, although the free energy difference between $\mathbf{CP_A}$ and $\mathbf{CP_B}$ is negligible, the large and slow intersolute rotational motion clearly distinguishes the two species, which can be one of the important characteristics of "incomplete mixing" of a binary mixture of methanol/water.

The solvent separated configurations (**SS**) appear in the region around r_{CC} = 5−7 Å and r_{OO} = 5−8 Å, respectively. **4d** belongs to these configurations. As in the $\mathbf{CP_A}$, no particular combination of r_{CC} and r_{OO} is preferred in **SS**, indicating that the configurations are more strongly determined by the nearby water dynamics than the intersolute interactions. A transition state from the contact pair to solvent separated configurations appears at a r_{CC} distance of 5.4 Å with the free energy barrier of 2 kcal/mol in Figure 1. The r_{CC} and r_{OO} distances of 5.5 and 5.1 Å in Figure 7 can be identified as the corresponding transition state $\mathbf{TS_2}$. It is emphasized that the $\mathbf{TS_2}$ connects the **SS** and $\mathbf{CP_A}$. The general feature of $\mathbf{TS_2}$ is depicted in Scheme 2. As the two methyl groups associate, at least one of the two hydrogen bonds between hydroxyl groups and water should be broken to form $\mathbf{CP_A}$, which is the origin of the free energy barrier in Figure 1. Mechanistically, it can be concluded that the isomerization between the $\mathbf{CP_A}$ and $\mathbf{CP_B}$ competes with the dissociation process between the $\mathbf{CP_A}$ and **SS**. Although the 2D PMF shows the existence of the two types of contact pairs, their relative populations are not apparent. In order to obtain the

dx.doi.org/10.1021/jp308936g | J. Phys. Chem. B 2012, 116, 14254−14260

quantitative distributions of the configurations, the trajectories of all umbrella sampling windows were searched for the structures of $\mathbf{CP_A}$, $\mathbf{CP_B}$, and **SS**. The results are presented in Figure 8. The clear distinction between the $\mathbf{CP_A}$ and $\mathbf{CP_B}$ can

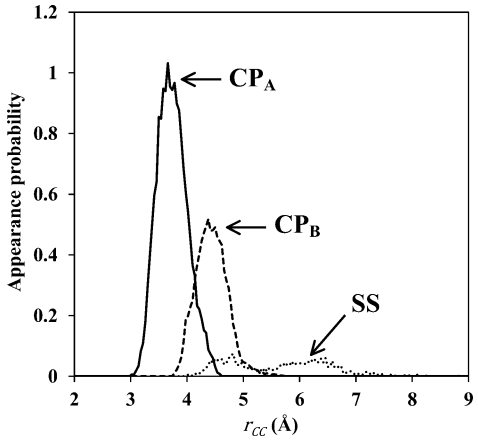

Figure 8. The relative populations of $\mathbf{CP_A}$, $\mathbf{CP_B}$, and **SS**. The intersolute r_{OO} and r_{CC} bond criteria were used in the characterizations of each species from the snapshot of MD simulations. The $\mathbf{CP_A}$ is defined as the intersolute C−H distance of methyl groups being below 3.5 Å. In the case of $\mathbf{CP_B}$, the intersolute O−H distance of hydroxyl groups being below 2.8 Å was the criteria. The solvent separated pair (**SS**) is defined as a structure where the solvent water has direct hydrogen bondings (2.8 Å criteria) with both methanols at the same time.

be seen with the $\mathbf{CP_A}$ having larger populations. This quantitative analysis again clearly shows the existence of two unique species in the contact pair regions. Relatively small populations of **SS** appear with r_{CC} distances of 4−7 Å.

IV. CONCLUSIONS

The association dynamics of methanol molecules in aqueous solution were theoretically studied with quantum mechanical/effective fragment potential-molecular dynamics (QM/EFP-MD) and *ab initio* quantum mechanical calculations. The umbrella sampling technique was adopted to obtain the potential of mean force (PMF) along the intermolecular distance of a methanol pair (r_{CC}). Two types of stable contact pairs of $\mathbf{CP_A}$ and $\mathbf{CP_B}$ were found, with a shallow second potential minimum of the solvent-separated configuration (**SS**). The stable contact pairs imply the strong association tendency of methanol molecules in aqueous solution, supporting the "incomplete mixing" theory. Our *ab initio* calculations on model clusters and the additional two-dimensional (2D) PMF further established that the $\mathbf{CP_A}$ and $\mathbf{CP_B}$ are formed by hydrophobic and hydrophilic attractions, respectively. The structural analysis of snapshots showed that the $\mathbf{CP_A}$ has a larger population.

Mechanistically, a mild transition state ($\mathbf{TS_1}$) of isomerization between $\mathbf{CP_A}$ and $\mathbf{CP_B}$ appears at around r_{CC} = 3.8 Å and r_{OO} =3.4 Å. Although the free energy difference between $\mathbf{CP_A}$ and $\mathbf{CP_B}$ and the associated free energy barrier of $\mathbf{TS_1}$ are negligible, the slow intersolute rotational motion of isomerization distinguishes the two species. A steep transition state $\mathbf{TS_2}$ connecting the hydrophobic $\mathbf{CP_A}$ and solvent separated **SS** exists at r_{CC} = 5.5 Å and r_{OO} = 5.1 Å. The origin of the free energy barrier of $\mathbf{TS_2}$ comes from the large structural changes between the $\mathbf{CP_A}$ and **SS**. This conversion of **SS** into $\mathbf{CP_A}$ by hydrophobic attraction initiates the association. After that, the hydrophilic attraction between hydroxyl groups of methanol molecules further converts $\mathbf{CP_A}$ into $\mathbf{CP_B}$. Our mechanism implies that the hydrophobic attraction between methyl groups operates on the longer intermolecular distance, while the hydrophilic attraction between hydroxyl groups is effective in contact pairs.

In summary, our study provides direct theoretical evidence and a detailed mechanism of the methanol/water "incomplete mixing" process. We show that not only the hydrophobic but also hydrophilic attractions between a methanol pair play an important role in the methanol solvation structures and their dynamics.

AUTHOR INFORMATION

Corresponding Author

*E-mail: cchoi@knu.ac.kr.

Notes

The authors declare no competing financial interest.

ACKNOWLEDGMENTS

This work was supported by the National Research Foundation of Korea (NRF) grant to C.H.C. funded by the Korea government (MEST) (No. 2007-0056341 and No. 2012-004812).

REFERENCES

(1) Widom, B.; Bhimalapuram, P.; Koga, K. *Phys. Chem. Chem. Phys.* **2003**, *5*, 3085−3093.
(2) Chandler, D. *Nature* **2005**, *437*, 640−647.
(3) Pratt, L. R. *Annu. Rev. Phys. Chem.* **2002**, *53*, 409−436.
(4) Wang, S. Q.; Humphreys, E. S.; Chung, S. Y.; Delduco, D. F.; Lustig, S. R.; Wang, H.; Parker, K. N.; Rizzo, N. W.; Subramoney, S.; Chiang, Y. M.; Jagota, A. *Nat. Mater.* **2003**, *2*, 196−200.
(5) Murrell, J. N.; Jenkins, A. D. *Properties of liquids and solutions*, 2nd ed.; John Wiley & Sons: New York, 1994.
(6) Frank, H. S.; Evans, M. W. *J. Chem. Phys.* **1945**, *13*, 507−532.
(7) Ludwig, R. *Chem. Phys.* **1995**, *195*, 329−337.
(8) Rossky, P. J.; Karplus, M. *J. Am. Chem. Soc.* **1979**, *101*, 1913−1937.
(9) Zichi, D. A.; Rossky, P. J. *J. Chem. Phys.* **1986**, *84*, 2814−2822.
(10) Sciortino, F.; Geiger, A.; Stanley, H. E. *Nature* **1991**, *354*, 218−221.
(11) Turner, J.; Soper, A. K. *J. Chem. Phys.* **1994**, *101*, 6116−6125.
(12) Sidhu, K. S.; Goodfellow, J. M.; Turner, J. Z. *J. Chem. Phys.* **1999**, *110*, 7943−7950.
(13) Fidler, J.; Rodger, P. M. *J. Phys. Chem. B* **1999**, *103*, 7695−7703.
(14) Van Erp, T.; Meijer, E. *Chem. Phys. Lett.* **2001**, *333*, 290−296.
(15) Gallagher, K. R.; Sharp, K. A. *J. Am. Chem. Soc.* **2003**, *125*, 9853−9860.
(16) Laage, D.; Hynes, J. T. *Science* **2006**, *311*, 832−835.
(17) Qvist, J.; Halle, B. *J. Am. Chem. Soc.* **2008**, *130*, 10345−10353.
(18) Laage, D.; Stirnemann, G.; Hynes, J. T. *J. Phys. Chem. B* **2009**, *113*, 2428−2435.
(19) Laage, D. *J. Phys. Chem. B* **2009**, *113*, 2684−2687.
(20) Silvestrelli, P. L. *J. Phys. Chem. B* **2009**, *113*, 10728−10731.
(21) Dixit, S.; Crain, J.; Poon, W. C. K.; Finney, J. L.; Soper, A. K. *Nature* **2002**, *416*, 829−832.
(22) Guo, J. H.; Luo, Y.; Augustsson, A.; Kashtanov, S.; Rubensson, J. E.; Shuh, D. K.; Ågren, H.; Nordgren, J. *Phys. Rev. Lett.* **2003**, *91*, 157401−157404.
(23) Møller, C.; Plesset, M. S. *Phys. Rev.* **1934**, *46*, 618−622.
(24) Adamovic, I.; Gordon, M. S. *J. Phys. Chem. A* **2006**, *110*, 10267−10273.
(25) Pratt, L. R.; Chandler, D. *J. Chem. Phys.* **1977**, *67*, 3683−3704.
(26) Young, W. S.; Brooks, C. L., III. *J. Chem. Phys.* **1997**, *106*, 9265−9269.

(27) Czaplewski, C.; Rodziewicz-Motowidlo, S.; Liwo, A.; Ripoll, D. R.; Wawak, R. J.; Scheraga, H. A. *Protein Sci.* **2000**, *9*, 1235−1245.
(28) Wensink, E. J. W.; Hoffmann, A. C.; van Maaren, P. J.; van der Spoel, D. *J. Chem. Phys.* **2003**, *119*, 7308−7317.
(29) Car, R.; Parrinello, M. *Phys. Rev. Lett.* **1985**, *55*, 2471−2474.
(30) Masunov, A.; Lazaridis, T. *J. Am. Chem. Soc.* **2003**, *125*, 1722−1730.
(31) Komeiji, Y.; Nakano, T.; Fukuzawa, K.; Ueno, Y.; Inadomi, Y.; Nemoto, T.; Uebayasi, M.; Fedorov, D. G.; Kitaura, K. *Chem. Phys. Lett.* **2003**, *372*, 342−347.
(32) Field, M. J.; Bash, P. A.; Karplus, M. *J. Comput. Chem.* **1990**, *11*, 700−733.
(33) Gao, J. *J. Chem. Phys.* **1998**, *109*, 2346−2354.
(34) Xie, W.; Orozco, M.; Truhlar, D. G.; Gao, J. *J. Chem. Theory Comput.* **2009**, *5*, 459−467.
(35) Gordon, M. S.; Fedorov, D. G.; Pruitt, S. R.; Slipchenko, L. V. *Chem. Rev.* **2012**, *112*, 632−672.
(36) Day, P. N.; Jensen, J. H.; Gordon, M. S.; Webb, S. P.; Stevens, W. J.; Krauss, M.; Garmer, D.; Basch, H.; Cohen, D. *J. Chem. Phys.* **1996**, *105*, 1968−1986.
(37) Day, P. N.; Pachter, R.; Gordon, M. S.; Merrill, G. N. *J. Chem. Phys.* **2000**, *112*, 2063−2072.
(38) Netzloff, H. M.; Gordon, M. S. *J. Chem. Phys.* **2004**, *121*, 2711−2714.
(39) Adamovic, I.; Gordon, M. S. *J. Phys. Chem. A* **2005**, *109*, 1629−1636.
(40) Bandyopadhyay, P.; Gordon, M. S. *J. Chem. Phys.* **2000**, *113*, 1104−1109.
(41) Arora, P.; Slipchenko, L. V.; Webb, S. P.; DeFusco, A.; Gordon, M. S. *J. Phys. Chem. A* **2010**, *114*, 6742−6750.
(42) Choi, C. H.; Re, S.; Feig, M.; Sugita, Y. *Chem. Phys. Lett.* **2012**, *539*−*540*, 218−221.
(43) Brooks, B. R.; Bruccoleri, R. E.; Olafson, B. D.; States, D. J.; Swaminathan, S.; Karplus, M. *J. Comput. Chem.* **1983**, *4*, 187−217.
(44) Grossfield, A. http://membrane.urmc.rochester.edu/content/wham, 2012.
(45) Zhu, F.; Hummer, G. *J. Comput. Chem.* **2011**, *33*, 453−465.
(46) Li, J.-L.; Car, R.; Tang, C.; Wingreen, N. S. *Proc. Natl. Acad. Sci. U.S.A.* **2007**, *104*, 2626−2630.